Γ_A = parameter defined by (24)
Γ_R = parameter defined by (25)
δ = thickness of liquid mass transfer film
ϵ = liquid holdup
θ = dimensionless residence time, defined by (18)
$\tilde{\rho}_l$ = molar density of liquid phase
τ = residence time

Subscripts

A = of species A
B = of species B
c = stream leaving condenser
f = feed stream
g = gaseous phase
i = gas-liquid interface
l = liquid phase
L = of species L
o = stream leaving reactor
R = of species R
S = of species S

LITERATURE CITED

Ding, J. S., Shanmuk Sharma, and Dan Luss, "Steady State Multiplicity and Control of the Chlorination of Liquid *n*-Decane in an Adiabatic Continuously Stirred Tank Reactor," *Ind. Eng. Chem. Fundamentals*, 13, 76 (1974).

Hoffman, L. A., M.S. thesis, "Theoretical Study of Steady State Multiplicity and Stability in Gas Liquid Continuous Stirred Tank Reactors," Univ. Houston, Tex. (1974).

———, Shanmuk Sharma, and Dan Luss, "Steady State Multiplicity of Adiabatic Gas-Liquid Reactors: 1. The Single Reaction Case," *AIChE J.*, **21**, 318 (1975).

Pangarkar, V. G., "Gas Absorption With Reaction in a Solution Containing a Volatile Reactant," *Chem. Eng. Sci.*, **29**, 877 (1974).

Schmitz, R. A., and N. R. Amundson, "An Analysis of Chemical Reactor Stability and Control—Two Phase Systems in Physical Equilibrium," *ibid.*, **18**, 265 (1963*a*).

———, "An Analysis of Chemical Reactor Stability and Control—Two Phase Gas-Liquid and Concentrated Liquid-Liquid Reacting Systems in Physical Equilibrium," *ibid.*, 391 (1963*b*).

———, "An Analysis of Chemical Reactor Stability and Control—Two Phase Chemical Reacting Systems with Heat and Mass Transfer Resistances," *ibid.*, 415 (1963*c*).

———, "An Analysis of Chemical Reactor Stability and Control—Two Phase Chemical Reacting Systems with Fast Reactions," *ibid.*, 447 (1963*d*).

Szekely, J., and J. Bridgwater, "Some Further Consideration on Mass Transfer and Selectivity in Fluid-Fluid Systems," *ibid.*, **22**, 711 (1967).

Teramoto, M., T. Nagayasu, T. Matsui, K. Hashimoto, and S. Nagata, "Selectivity of Consecutive Gas Liquid Reactions," *Chem. Eng. Japan*, **2**, 186 (1969).

Van Krevelen, D. W., and P. J. Hoftijzer, "Kinetics of Gas Liquid Reactions—General Theory," *Rec. Trav. Chim. Pays-Bas*, **67**, 563 (1948).

Westerterp, K. R., "Maximum Allowable Temperatures in Chemical Reactors," *Chem. Eng. Sci.*, **17**, 423 (1962).

Manuscript received September 18, 1975; revision received and accepted September 28, 1975.

Mathematical Models of the Monolith Catalytic Converter:

LARRY C. YOUNG

and

BRUCE A. FINLAYSON

Department of Chemical Engineering
University of Washington
Seattle, Washington 98195

Part I. Development of Model and Application of Orthogonal Collocation

The orthogonal collocation method is applied to solve the mathematical model of a monolith catalytic converter, in which the reaction takes place in a porous catalytic layer deposited on the wall of a tube. A sequence of models is developed, with the most complicated one involving transient heat and mass transfer in three dimensions.

SCOPE

The orthogonal collocation method is developed for application to problems having irregular geometries. Most previous applications of orthogonal collocation in two dimensions have been for rectangular regions (Villadsen and Stewart, 1967; Sørensen et al., 1973; Young and Finlayson, 1973). A notable exception is the series of papers by Sørenson and Stewart (1974) dealing with flow of a fluid in a packed bed. In the applications to monolith catalytic reactors envisaged below, the duct frequently takes irregular shapes. Consequently, it is necessary to apply orthogonal collocation in these irregular three-dimensional geometries.

The monolith reactor is a large number of small, long tubes (in parallel) through which a gas flows, and catalyst is deposited on a porous layer on the wall of the duct. Another important objective is model discrimination; different mathematical models are developed for such devices in order to illustrate the phenomena oc-

curring in them and to determine the simplest, correct model. Current models of catalytic mufflers for oxidation of carbon monoxide in automobile exhaust approximate the transverse diffusion and conduction in the fluid by means of assigned Nusselt and Sherwood numbers (Kuo, 1973; Hegedus, 1974; Votruba et al., 1975). One objective of the study is to test this assumption to see its limitations, since the calculations of Young and Finlayson (1974) suggest that the assumption may not always be valid. Another important feature of the model is the effect of axial conduction in the wall, since Eigenberger (1972) has shown that the inclusion of axial conduction may drastically alter both the steady state and transient behavior of packed beds. Models are developed with and without axial conduction so that this effect can be examined. Finally, peripheral diffusion and conduction is included in one model to see its effect.

The equations for the various models are written down, and then the details of application of the orthogonal collocation method are given. The novel features of the analysis are the method of handling irregular geometry, which makes possible calculations for a variety of ducts with different shapes with one computer program; and the rearrangement of the fluid mass and energy transport problem by using Graetz problems, which drastically reduces the total number of unknowns in the approximate solution. Both extensions of the orthogonal collocation method make possible the efficient calculations whose results are given in Part II as applied to automobile exhaust.

CONCLUSIONS AND SIGNIFICANCE

A number of important conclusions are obtained relative to the application of the orthogonal collocation method. The average energy equation (or mass balance) is satisfied exactly by the approximate solution if there are no quadrature points on the boundary. Graetz problems for two-dimensional irregularly shaped ducts are solved by using the orthogonal collocation method after transformation of the domain. Quadrature formulas are given for integrals over the cross section of a duct and on the boundary of the duct, and the proper choice of collocation points is given for the transformed domains.

Graetz problems are solved for various geometries, mainly because the results were used in the solution method of the monolith models. However, more accurate results are obtained for the asymptotic Nusselt number in a constant temperature Graetz problem for the following geometries: square, rectangles with aspect ratio of 0.5 and 0.25, and equilateral triangles. An asymptotic formula is given for the Nusselt number near the inlet of the duct. New results are obtained for two trapezoid geometries: friction factor and asymptotic Nusselt number for boundary conditions of constant temperature and linearly varying wall temperature.

Mathematical models are developed for monolith chemical reactors, including transport of heat and mass in the fluid, axial conduction and diffusion in the wall or porous layer, peripheral conduction or diffusion in the wall or porous layer, and laminar flow of the fluid. Simplifications of these models permits elimination of each of these phenomena in order to test their importance.

Solution of the mathematical model by orthogonal collocation is feasible and extremely useful. When axial conduction in the wall is included, orthogonal collocation on finite elements is used. When the distribution of temperature and concentration in the fluid is important, a technique is given for reducing the complexity of the problem and greatly reducing the number of unknowns (by factors ranging from 3 to 15). It is possible to handle irregular geometries by using fairly general methods after transformation of the domain, so that it is possible to examine the influence of geometry on converter performance by using the same computer program.

AVERAGE ENERGY EQUATION

One choice to be made in the collocation method is the location of the collocation points. A certain choice is preferable to others as we illustrate by examining the problem of heat transfer to a duct wall when a fluid flows in laminar flow through a pipe with circular cross section. The governing dimensionless equations for a specified wall heat flux are

$$(1-x^2)\frac{\partial T}{\partial z} = \frac{1}{x}\frac{\partial}{\partial x}\left(x\frac{\partial T}{\partial x}\right) \tag{1}$$

$$T(0,x) = T_O, \quad \left.\frac{\partial T}{\partial x}\right|_{x=0} = 0 \tag{2}$$

$$\left.\frac{\partial T}{\partial x}\right|_{x=1} = h(z) \tag{3}$$

The mixing cup temperature is

$$T^M(z) = 4\int_o^1 (1-x^2)T(z,x)x\,dx \tag{4}$$

and the local Nusselt number is defined in two ways:

$$Nu(z) = \frac{-2}{T^M - T(z,1)}\left.\frac{\partial T}{\partial x}\right|_{x=1} \tag{5}$$

$$Nu(z) = \frac{-0.5}{T^M - T(z,1)}\frac{dT^M}{dz} \tag{6}$$

The first definition is the standard one, and the second results from use of the average energy equation, found by integrating Equation (1) in x:

$$4\left.\frac{\partial T}{\partial x}\right|_{x=1} = \frac{dT^M}{dz} \tag{7}$$

This leads to the boundary condition

$$\frac{1}{4}\frac{dT^M}{dz} = h(z) \tag{8}$$

One would like the average energy equation to be satisfied exactly, but this does not happen for all approximation techniques.

In the application of orthogonal collocation to these equations, a solution of the following form is assumed:

$$T(x,z) = \sum_{j=1}^{N+1} L_j(x^2)T(x_j,z) \tag{9}$$

where $L_j(x^2)$ is the Lagrange interpolating polynomial. The analyst has the freedom to choose the N interior collocation points x_i. The collocation points are usually taken as the roots of a Jacobi polynomial, defined by

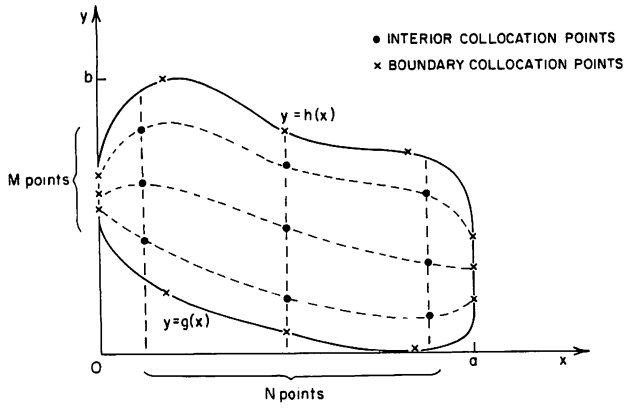

Fig. 1. Two-dimensional arrangement of collocation points for an irregular domain, · interior collocation points, x boundary collocation points.

$$\int_o^1 x^{2i-2} P_N(x^2)\, w(x^2)\, x\, dx = 0 \text{ for } i = 1, \ldots, N \tag{10}$$

Either $w(x^2) = 1$ or $w(x^2) = 1 - x^2$ is commonly used. For $w(x^2) = 1$, the polynomial roots are the base points of the Gaussian quadrature formula, while $w(x^2) = 1 - x^2$ gives the base points of the Radau quadrature formula (Krylov, 1962). Both quadrature formulas are of the form

$$\int_o^1 f(x^2)\, x\, dx = \sum_{j=1}^{N+1} W_j f(x_j^2) \tag{11}$$

For the Gaussian quadrature, the formula (11) is exact for $f(x^2)$, a polynomial of degree $2N - 1$ or less in x^2, and the weight factor on the boundary is zero, $W_{N+1} = 0$. For the Radau quadrature, the formula is exact for polynomials of degree $2N$ or less in x^2 and $W_{N+1} \neq 0$.

Numerical experience has established guidelines on the best choice of points between these two (Ferguson, 1971). The best choice depends on the type of boundary condition. If the boundary condition is of the first kind, solution specified on the boundary, then Radau quadrature base points usually give slightly better results than Gaussian points. If the boundary condition is of the second or third kind, then Gaussian points give substantially better results than Radau points. If Radau points are used with second or third kind boundary conditions, then an integrated form of the boundary condition must be used to achieve reasonable accuracy and convergence (Ferguson, 1971; Elnashaie and Cresswell, 1973; Ferguson and Finlayson, 1974).

That the best choice of collocation points are quadrature base points is no coincidence, since this choice enables one to achieve accurate approximations of other weighted residual methods. Young (1974) has shown that the best approximation to the moments and least-squares methods results when Gaussian quadrature base points are used, regardless of the boundary conditions. The best approximation to the Galerkin method results by using Radau points for first kind boundary conditions and Gaussian points for second or third kind boundary conditions. Interestingly, numerical experience suggests that for the general case one should use the points which best approximate the Galerkin method; however, for specific cases other choices might give slightly better results.

Next we apply orthogonal collocation to the heat transfer equation. The differential equation is

$$(1 - x_j^2)\frac{dT_j}{dz} = \sum_{i=1}^{N+1} B_{ji} T_i \quad j = 1, \ldots, N \tag{12}$$

The boundary condition, Equation (3), is

$$\sum_{i=1}^{N+1} A_{N+1,i} T_i = h(z) \tag{13}$$

where

$$A_{ij} = \left.\frac{dL_j(x^2)}{dx}\right|_{x_i} \quad \text{and} \quad B_{ij} = \left.\frac{d^2 L_j(x^2)}{dx^2}\right|_{x_i}$$

If we wish to use the boundary condition in the form of Equation (8), we need

$$\frac{dT^M}{dz} = \frac{\sum_{j=1}^{N+1} W_j(1 - x_j^2)\frac{dT_j}{dz}}{\sum_{j=1}^{N+1} W_j(1 - x_j^2)} = 4\sum_{j=1}^{N+1} W_j(1 - x_j^2)\frac{dT_j}{dz} \tag{14}$$

Since the term for $x_{N+1} = 1.0$ drops out ($W_{N+1} = 0$) by virtue of Equation (12), we can write

$$\frac{dT^M}{dz} = 4\sum_{j=1}^{N} W_j \sum_{i=1}^{N+1} B_{ji} T_i \tag{15}$$

The boundary condition (8) is then

$$\sum_{i=1}^{N+1} T_i \sum_{j=1}^{N} W_j B_{ji} = h(z) \tag{16}$$

It is a general result that

$$\sum_{j=1}^{N+1} W_j B_{ji} = A_{N+1,i} \tag{17}$$

so that if $W_{N+1} = 0$ Equations (16) and (13) are identical. Thus we see that the average energy equation (7) is satisfied by the approximation provided $W_{N+1} = 0$. This is true for the Gaussian quadrature points ($w = 1$) but not for the Radau quadrature points ($w = 1 - x^2$).

In problems of reaction and diffusion, the average mass balance is satisfied if Gaussian quadrature points are used but not if Radau quadrature points are used. If Radau points are used, in order to reduce errors arising from the boundary condition, Equation (3), the boundary condition can be rewritten in integral form, as was done for Equation (8); however, in other problems this procedure is more difficult. This has been noted previously by Ferguson (1971), Elnashaie and Cresswell (1973) and Ferguson and Finlayson (1974). It is more convenient and as accurate to simply use the Gaussian quadrature points ($w = 1$). The same conclusion applies if the geometry is spherical or planar.

GRAETZ PROBLEM IN TWO DIMENSIONS

Consider a two-dimensional figure as shown in Figure 1. In order to achieve accurate approximations, we wish to define optimal quadrature formulas for integrals over the surface $dS = dx\, dy$ and on the boundary, dl:

$$\int_s f(x, y)\, dS = \sum_{i=1}^{N} W_i f(x_i, y_i) \tag{18}$$

$$\int_c f(l)\, dl = \sum_{i=1}^{N} W_i' f(l_i) \tag{19}$$

Stroud (1971) discusses both product and nonproduct quadrature formulas similar to Equation (18).

Product formulas are constructed by transforming the independent variables and by writing the integral (18) as a double integral:

$$\int_S f(x,y)\,dS = \int_0^1 \int_0^1 f(\xi,\eta)\,[h(a\xi) - g(a\xi)]\,d\eta\,a\,d\xi \tag{20}$$

where

$$\eta = \frac{y - g(x)}{h(x) - g(x)},\quad \xi = \frac{x}{a} \tag{21}$$

The quadrature weights and base points can be determined from the theory of quadrature in one dimension. The optimal base points η_j are simply the Gaussian quadrature points defined by

$$\int_0^1 \eta^{i-1} P_M(\eta)\,d\eta = 0,\ i = 1, \ldots, M \tag{22}$$

The optimal base points ξ_i are the roots of the N^{th} degree orthogonal polynomial defined by

$$\int_0^1 \xi^{i-1} P_N(\xi)\,[h(a\xi) - g(a\xi)]\,d\xi = 0,\ i = 1, \ldots, N$$

The resulting quadrature formula is

$$\int_S f(x,y)\,ds = \sum_{i=1}^{N} \sum_{j=1}^{M} W_i^{\xi} W_j^{\eta} f(\xi_i, \eta_j) \tag{24}$$

and will be exact when f is a polynomial of degree $2N - 1$ or less in ξ and $2M - 1$ or less in η. All quadrature points lie on the interior of the region. A two-dimensional Radau quadrature formula can be generated, in which case the additional factors $\eta(1 - \eta)$ and $\xi(1 - \xi)$ are included in Equations (22) and (23), respectively. If the problem is symmetric in ξ or η, the polynomials can be defined to include this symmetry [compare Equation (22) with (10)]. In the standard application of collocation procedures, the polynomials themselves need not be found; only the quadrature points are needed, and these are often available (Stroud and Secrest, 1966).

The subject of optimal nonproduct quadrature schemes is not well developed (Stroud, 1971, p. 91). In nonproduct quadrature schemes, a total of N quadrature points might be placed inside (or sometimes outside) the region shown in Figure 1, without regard for obtaining a regular pattern, which is essential to the use of Lagrange interpolation. There are several nonproduct formulas for some of the regions for which theory has been developed (Stroud, 1971). For the square, one of the nonproduct formulas happens to be a product formula. Owing to insufficient information to guide our choice, here we restrict attention to product formulas.

The surface integral is then Equation (24), while the line integral is

$$\int_C f\,dl = \int_0^1 f\sqrt{1 + (g')^2}\,a\,d\xi + \int_0^1 f\sqrt{1 + (h')^2}\,a\,d\xi$$
$$+ [h(0) - g(0)] \int_0^1 f\,d\eta + [h(a) - g(a)] \int_0^1 f\,d\eta$$
$$= \sum_{i=1}^{N_g} W_i^g f(a\xi_i^g),\ g(a\xi_i^g) + \sum_{i=1}^{N_h} W_i^h f(a\xi_i^h),\ h(a\xi_i^h)$$
$$+ \sum_{i=1}^{N_3} W_i^0 f[0, g(0)\ (1 - \eta_i) + \eta_i h(0)]$$
$$+ \sum_{i=1}^{N_4} W_i^a f[a, g(a)\ (1 - \eta_i) + \eta_i h(a)] \tag{25}$$

The base points η_i are defined as shown above, Equation (22), while the optimal base points ξ_i^g and ξ_i^h are the roots of orthogonal polynomials defined by (Krylov, 1962, p. 161):

$$\int_0^1 \xi^{i-1} P_{N_r}{}^r(\xi) \sqrt{1 + [r'(a\xi)]^2}\,d\xi = 0,\ i = 1, \ldots, N^r$$
$$r = h \text{ or } g$$

Special procedures must be used when g' or h' are infinite. If the problem has a symmetry about $x = \frac{1}{2}$ or $y = \frac{1}{2}$, the line of symmetry can be used as one boundary, thus reducing the number of collocation points.

Having thus determined the quadrature points, we use them as collocation points, since this gives an accurate approximation to other weighted residual methods. We transform the coordinate system (x, y) to (ξ, η) using Equation (21). Then derivatives change as follows:

$$a\frac{\partial T}{\partial x} = \frac{\partial T}{\partial \xi} + a(y\hat{h}' - \hat{g}')\frac{\partial T}{\partial \eta} \tag{27}$$

$$\hat{h}(x) = [h(x) - g(x)]^{-1},\ \hat{g}(x) = g(x)\,\hat{h}(x) \tag{28}$$

$$a\frac{\partial T}{\partial y} = a\hat{h}\frac{\partial T}{\partial \eta} \tag{29}$$

and so forth. The normal unit vectors are

$$\mathbf{n} = \frac{-\mathbf{e}_x h' + \mathbf{e}_y}{\sqrt{1 + (h')^2}} \text{ on } y = h \tag{30}$$

$$\mathbf{n} = \frac{\mathbf{e}_x g - \mathbf{e}_y}{\sqrt{1 + (g')^2}} \text{ on } y = g \tag{31}$$

Using the above relations, we can write the differential equations and boundary conditions in terms of ξ on η derivatives. Orthogonal collocation is applied by taking, for example

$$\left.\frac{\partial^2 T(\xi,\eta)}{\partial \eta^2}\right|_{\xi_k,\eta_j} = \sum_{i=1}^{N+2} B_{ji}^{\eta} T(\xi_k, \eta_i) \tag{32}$$

where the B matrix is the usual matrix representing the second derivative (Finlayson, 1972).

By using the above procedures, Graetz problems have been solved for a variety of geometries. We report here only new or more accurate results; other calculations confirmed that the results were comparable to literature values when available. The velocity is found by solving

$$8r_h^2 \nabla_{II}^2 G = -1 \text{ in } S,\ G = 0 \text{ on } C \tag{33}$$

$$\nabla_{II}^2 = \frac{\partial^2}{\partial x^2} + \frac{\partial^2}{\partial y^2} \tag{34}$$

and the desired feature of the solution is the friction factor times the Reynolds number $fRe = 1/\langle G \rangle$. The brackets denote an average over S:

$$\langle G \rangle = \frac{\int_S G\,dx\,dy}{\int_S dx\,dy} \tag{35}$$

The temperature is the solution of

$$\frac{G(x,y)}{\langle G\rangle}\frac{\partial T}{\partial z} = 8r_n^2\nabla_{II}^2 T \quad z>0 \qquad (36)$$

$$(x,y) \text{ in } S$$

$$T(x,y,z=0) \qquad (37)$$

under various types of boundary conditions:

$$\text{I} \quad T_o = 1, \quad T = 0 \text{ on } C \qquad (38)$$

$$\text{II} \quad T_o = 0, \quad T = z \text{ on } C \qquad (39)$$

For the more general boundary condition, $T = f(z)$ on C, the eigenvalues and other constants needed to calculate solutions are given by Young (1974). The desired quantity is the Nusselt number averaged around the periphery. With the definitions

$$T^M \equiv \int_S GTdS / \int_S GdS \qquad (40)$$

and

$$\{f\} \equiv \int_C f\,dl / \int_C dl \qquad (41)$$

we want

$$\langle Nu\rangle = \frac{-4r_h\{\underline{n}\cdot\nabla T\}}{T^M - \{T\}} \qquad (42)$$

The asymptotic value $\langle Nu_\infty\rangle$ occurs for $z \to \infty$.

For rectangular regions, solutions are available in Shah and London (1971). The value of the friction factor-Reynolds number product fRe and the asymptotic Nusselt number under boundary conditions II are evaluated by using up to thirty terms of the exact representation by an infinite series. Calculations with orthogonal collocation were made with symmetric polynomials in x and y, that is, those defined by Equation (9) with $w = 1$. The results agreed with the exact results to six digits, with small differences in the seventh digit. For the square duct, the number of terms used was $N = M = 6$, while for an aspect ratio of 0.5 and 0.25, we used $N = 4$ (in the direction of the short dimension) and $M = 7$. Since symmetric trial functions were used, only a quadrant was solved for the rectangle, and only half of the quadrant was solved for the square, which has additional symmetry. For the boundary condition of type I, the most accurate results presented by Shah and London are from an unpublished paper which utilized a finite difference method and reported values of the asymptotic Nusselt number to four digits. Our results show convergence to within four to six digits as N and M are increased (Young, 1974). Thus we regard the asymptotic values listed in Table 1 as the most accurate available.

For the Graetz problem in a circle, Sellars et al. (1956) showed that the Nusselt number in the entry length follows the formula

$$\langle Nu\rangle = az^{-1/3} \qquad (43)$$

where the constant a is determined by the Leveque solution. The power on z is dictated by the boundary layer type of solution at the inlet, and this power should be the same in all geometries. Calculations by us and others (Shah and London, 1971) confirm this, and the appropriate constants for rectangular ducts are given in Table 2.

The collocation method was applied to the Graetz problem for an equilateral triangular duct for comparison purposes. In that case $h(x) = bx$ and $g(x) = 0$. Various quadrature points (collocation points) were used corresponding to different weighting functions. When $N = 6$ and $M = 3$ were used, the Nusselt numbers at $z = 0.01$ varied with the different weighting functions by ±5%, but the asymptotic Nusselt number differed only in the fourth digit for the different weighting functions. The value obtained was 2.491. This is probably more accurate than that given by Shah and London (1971) who report values ranging from 2.35 to 2.70, with 2.47 as the preferred value.

Two trapezoidal duct cases were studied: $b = 1$, $c = \frac{1}{2}$, and $b = \frac{3}{4}$, $c = \frac{1}{4}$. A weight function of 1 was used in both ξ and η. The collocation points for the case $N = 6$ and $M = 4$ are illustrated in Figure 2 for one of the trapezoids. Values of fRe and asymptotic Nusselt numbers are listed in Table 3 as derived with $N = 6$, $M = 4$. The complete results suggest that these values are correct to five digits. The developing profiles were also derived, and the eigenvalues and constants needed to

Table 1. Asymptotic Nusselt Numbers for Constant Wall Temperature

Geometry	Orthogonal collocation N	M	$\langle Nu_\infty\rangle$	Shah and London (1971) $\langle Nu_\infty\rangle$
Square, $b/a = 1$	6	6	2.977524	2.976
Rectangle, $b/a = 0.5$	4	7	3.3923	3.391
$b/a = 0.25$	4	7	4.4405	4.439
Equilateral triangle	3	6	2.491	2.47

Table 2. Nusselt Number Near the Inlet

Geometry	Aspect ratio	Parameter a in Equation (43)* Constant temperature	Linear wall temperature
Square	1.0	1.16	1.79
Rectangle	0.5	1.23	1.89
	0.25	1.38	2.05
Equilateral triangle		0.860	—

* Formula (43) is valid for $z < 0.01$.

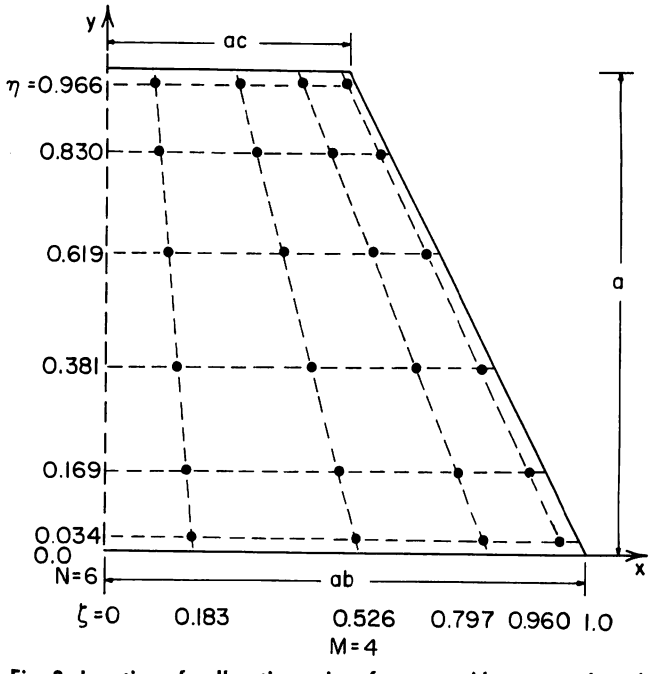

Fig. 2. Location of collocation points for trapezoid.——— boundary, - - - line of symmetry.

Table 3. Friction Factors and Asymptotic Nusselt Numbers for Trapezoidal Ducts

Geometry	fRE	Constant wall temperature $<Nu_\infty>$	Linear wall temperature $<Nu_\infty>$
$b = 1.0,\ c = 0.5$	14.192	2.8764	3.5279
$b = 0.75, c = 0.25$	13.9057	2.7736	3.404

calculate the solution for other wall temperature distributions are given elsewhere (Young, 1974). The fully developed condition is reached at $z = 0.1$, so that for lengths longer than this, the asymptotic Nusselt number holds.

MATHEMATICAL MODEL FOR MONOLITH

The convective transport of heat and mass is governed by the equations of motion, energy, and continuity. The complete set of equations are given by Bird et al. (1960, Chapt. 18), and these are simplified below for application to the monolith converter.

The flow of exhaust gas through the monolith cells is not of prime importance in itself, but only insofar as it affects heat and mass transfer in the device. Of utmost importance is whether flow is in the laminar or turbulent regime. For a typical engine, the flow rate will vary from 0.01 at idle to 0.05 std. m^3/s or more at highway cruising speeds. For typical converters, the Reynolds number will then vary between 75 and 600. Since the transition to turbulent flow for many duct shapes occurs at approximately 2 000 (Knudsen and Katz, 1958), the flow is laminar.

Since the flow is laminar, heat and mass transfer between the exhaust gas and the monolith cell wall is similar to that in the Graetz problem. The axial diffusion of mass and heat in the fluid may be neglected for Peclet numbers greater than 50 (Hennecke 1968; Michelsen and Villadsen, 1974; Sorensen and Stewart, 1974), which is the case here. Another difference is that in the Graetz problem the velocity is usually fully developed, while in the monolith the velocity profile develops as the gas passes through the converter.

In a monolith converter, when the reaction rate is very fast, the reaction lights off at the converter inlet, and the converter is controlled solely by mass and heat transfer limitations. For this limiting case, mass transfer is governed by the Graetz problem with a constant reactant wall concentration of zero and a constant wall temperature equal to the adiabatic temperature. This Graetz problem has been solved for circular geometry by using both the fully developed velocity profile and the developing velocity profile. The results are summarized by Shah and London (1971). Since in this limiting case the reaction zone is at the inlet, where the velocity profile develops, the comparison of these Graetz problems will show the maximum effect of the developing velocity profile. The maximum error in the mixing cup average conditions is only 7% (Young, 1974); so it appears reasonable to assume that the velocity profile is fully developed throughout the converter.*

The equations of change would, of course, apply to the fluid in each cell of the monolith and to the entire monolith solid. It is advantageous to use the symmetry of the cell configurations, since in a monolith converter

* In much of the heat transfer literature on circular ducts, there is a factor of 2 error in the dimensionless axial coordinate. This has been corrected in the above comparison.

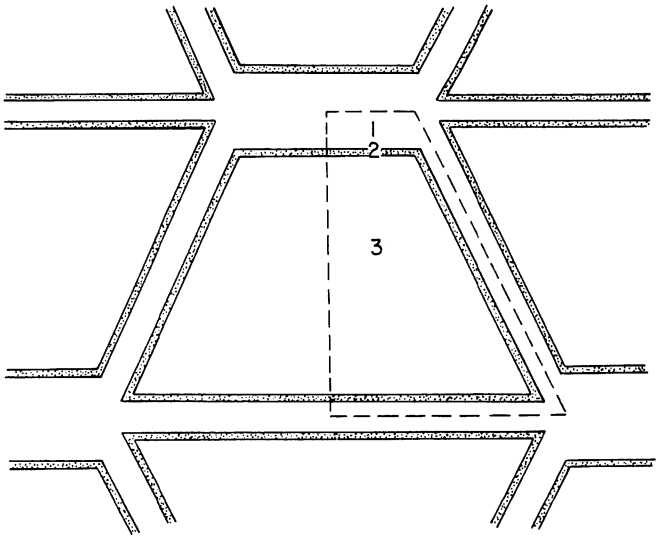

Fig. 3. Cross section of trapezoidal shaped duct. Region 1—substrate, 2—wash coat of porous material with catalyst, 3—fluid, - - - - region of calculation.

there are from one to five thousand cells. It would be a huge computational task to model every cell in the converter. Only the repetitive symmetric portion of the cells needs to be modeled if the converter is adiabatic and the flow rate is equal in all cells. Experimental evidence shows that the flow rate is not the same in each cell (Lemme and Givens, 1974; Howitt and Sekella, 1974), although Morgan et al. (1973) measured only minor radial temperature variations even during transient experiments. A nonuniform flow distribution between the cells tends to decrease the effectiveness of the converter under a given set of conditions. It is desirable to minimize flow variations, and considerable progress has been made in this direction. Since the radial temperature gradients are not large and flow straightening devices should be used, it appears reasonable to assume the conditions are the same in each cell, so that the symmetry of the device can be used.

By the nature of the problem, any mathematical model must be a transient one. It appears reasonable, however, to neglect some of the transient terms as in analysis of packed-bed reactors (Ferguson and Finlayson, 1974). Since monolith converters are somewhat similar, these criteria are used here. The thermal accumulation term for the fluid is neglected, since the ratio of fluid to solid thermal capacity is approximately 0.0007. The mass accumulation term for the fluid is neglected, since the residence time in the converter is from 0.003 to 0.02 s, while the thermal time constant is approximately 2 s. The transient response of velocity is neglected since velocity changes will occur on the order of $t = 1.8\ r_h^2\rho/\mu \simeq 0.002$ s (Bird et al., 1960, Chapt. 4). The transient response of mass in the catalytic layer can be neglected when the ratio of thermal to mass time constants is large. For the monolith converter, this ratio is approximately 10^5, which is substantially larger than the necessary ratio of 1 suggested by Ferguson and Finlayson (1974) for packed-bed reactors. This last effect, however, is included in some of the models, since no additional effort is required to do so.

The models developed below for the monolith converter embody the assumptions discussed above. There are, however, other phenomena which might be neglected, although there is no previous work which relates to these possible assumptions. To determine this information is one of the primary reasons for the present study.

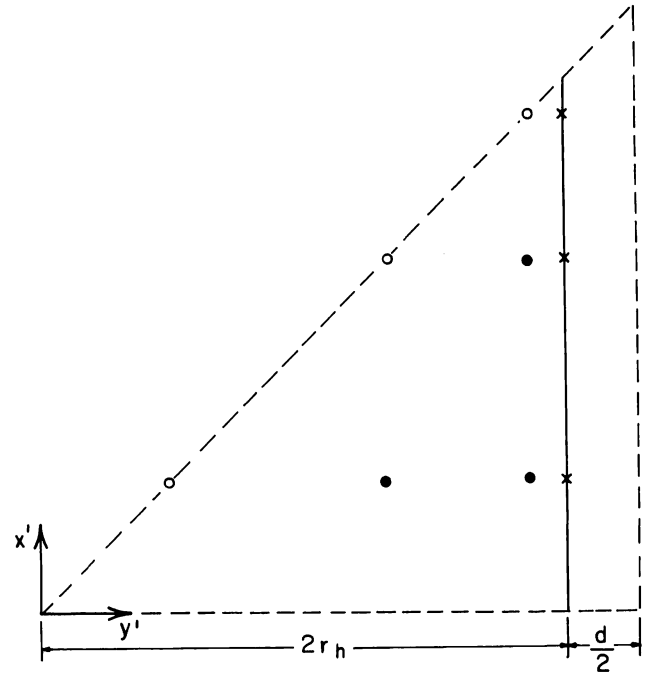

Fig. 4. Location of collocation points for square duct. --- line of symmetry, · interior collocation points, x solid boundary collocation points, ○ points of symmetry.

A series of models with various combinations of additional assumptions are developed below, so that the important features of the problem can be determined.

In order to specify a converter model, models must be chosen for heat and mass transfer in the three regions shown in Figure 3. The discussion below treats, in turn, heat and mass transfer in the fluid phase, heat transfer in the solid phase, and mass transfer in the catalytic layer.

Two models are developed to govern heat and mass transfer in the fluid. The first accounts for the distribution of heat and mass in the cell cross section, and the second assumes that heat and mass transfer coefficients may be used to account for the resistance to transfer between the fluid and the wall.

In the governing equations for the fluid, diffusion coupling is neglected, and an effective multicomponent diffusivity is used (Bird et al., 1960, Chapt 18). The fluid properties are assumed to be constant in the cell cross section; the gas is ideal with a constant average molecular weight. The compression work term is neglected in the energy equation, and no reaction is assumed to occur in the fluid. Under the above assumptions, the equations governing the fluid are

Heat, mass, and momentum balances for fluid in models II, II-A, and III-A

$$\frac{\partial T^f}{\partial z} = \alpha_1 \frac{8r_h^2 <G'>}{G'(x,y)} \nabla_{II}^2 T^f \tag{44}$$

$$\frac{\partial Y_i^f}{\partial z} = \alpha_2^i \frac{8r_h^2 <G'>}{G'(x,y)} \nabla_{II}^2 Y_i^f \tag{45}$$

$$8r_h^2 \nabla_{II}^2 G' = 8r_h^2 \frac{C}{\mu L} \frac{dP}{dz} \tag{46}$$

In Equations (44) and (45), the fluid properties may vary axially and with time, either explicitly or as a function of temperature and composition; however, in the calculations α_1 and α_2^i are assumed to be constant, since they vary by only 15% over a 400°F temperature change. The molar velocity G' is zero at the converter wall, and the boundary conditions for the fluid energy and continuity equations are determined by the equations governing the converter wall.

Simplified fluid equations are derived by integrating the fluid equations (44) and (45) across the fluid cross section and by defining Nusselt and Sherwood numbers in the usual way. With this assumption, the equations for the fluid become

Heat and mass balances for fluid in Models I and I-A

$$\frac{\partial T^M}{\partial z} = 2\alpha_1 Nu(T^s - T^M) \tag{47}$$

$$\frac{\partial Y_i^M}{\partial z} = 2\alpha_2^i Sh(Y_i^s - Y_i^M) \tag{48}$$

Equations (44) and (45) and (47) and (48) are designated as distributed and lumped parameter fluid models, respectively. If the Nusselt and Sherwood numbers in (47) and (48) are calculated from the solution to (44) and (45), then the two models will agree exactly for any wall temperature and composition distribution. The essential difference between the fluid models are that if Equations (44) and (45) are not solved, then the Nusselt and Sherwood numbers must be specified a priori, even though they may vary with position and time.

Three different models are considered for heat transfer in the solid phase. They differ by the conduction terms neglected in the three-dimensional transient heat conduction equation. To model the transfer of heat within the converter wall, the reaction is assumed to take place in an infinitesimal region at the fluid-solid interface. This assumption results, since the catalytic layer is thin (~0.025 mm) relative to the substrate (~0.25 mm), and the Prater relation (Smith, 1970, p. 446) suggests that the temperature change within the catalytic layer will be less than 1 deg. The catalytic layer and the substrate are assumed to have the same thermal diffusivity. In addition, the temperature is assumed to be constant in the direction perpendicular to the wall. An analysis by Young (1974) suggests that this assumption is valid provided $r_h k^s / r_{hs} k^f > 20$. In the monolith converter, this quantity is about 50, so the assumption appears justified.

The most complex and comprehensive model for heat transfer in the solid results by the application of the above assumptions to the transient three-dimensional heat conduction equation. The resulting equations are listed below for the square cell monolith, since this is the only geometry for which this model is solved:

Energy balance for solid in model III-A

$$\alpha_5 \left[\alpha_3 \frac{\partial T^s}{\partial t} - \left(\frac{r_{hs}}{L}\right)^2 \frac{\partial^2 T^s}{\partial z^2} - \left(\frac{r_{hs}}{2r_h + d/4}\right)^2 \frac{\partial^2 T^s}{\partial x^2} \right] + 2r_h \mathbf{n} \cdot \nabla T^f + \sum_{i=1}^{\hat{m}} \beta_5^i <r_i> = 0 \tag{49}$$

where $x = x'/2r_h$ for the coordinate system in Figure 4 and $<r_i>$ is the average reaction rate across the catalytic layer. The term $2r_h + d/4$ in Equation (49) is the average length of the wall in Figure 4. Similar equations can be derived for other cell geometries.

The second model considered for heat transfer in the solid is derived from that above by assuming that heat conduction is sufficiently fast that no appreciable temperature gradients develop around the periphery. Under this assumption, the governing equation for any geometry becomes

Energy balance for solid in models I-A and II-A

$$\alpha_5 \left[\alpha_3 \frac{\partial T^s}{\partial t} - \left(\frac{r_{hs}}{L}\right)^2 \frac{\partial^2 T^s}{\partial z^2} \right] + 2r_h (\mathbf{n} \cdot \nabla T^f)$$

$$+ \sum_{i=1}^{\hat{m}} \beta_5^i \langle r_i \rangle = 0 \quad (50)$$

In Equation (50), T^s is understood to be constant around the cell periphery.

The simplest model considered for the solid results by the additional assumption that heat conduction in the axial direction is zero. In this case, the governing equation becomes

Energy balance for solid in models I and II

$$\alpha_3\alpha_5 \frac{\partial T^s}{\partial t} + 2r_h(\mathbf{n}\cdot\nabla T^f) + \sum_{i=1}^{\hat{m}} \beta_5^i \langle r_i \rangle = 0 \quad (51)$$

By comparing the results predicted by the above three models, one can determine the importance of heat conduction around the periphery and axially. Radiation effects should probably be included and would cause effects similar to those caused by axial conduction.

The usual equation for modeling reaction and diffusion in a porous catalytic slab is

$$\frac{d^2Y_i^s}{d\xi^2} + \beta_4^i r_i = 0$$

$$Y_i^s(1) = Y_i^f; \quad \frac{dY_i^s(0)}{d\xi} = 0 \quad (52)$$

Equation (52) is, of course, a special case of the equation for three-dimensional transient diffusion and reaction. It assumes that the mass transient term can be neglected and that negligible diffusion takes place in the other two spatial directions. The mass transient term can be neglected, as discussed above, but there is no evidence to suggest that diffusion axially and around the periphery can be neglected.

For the above reasons, the following equation is the most complex model used to describe the catalytic layers, region 2 in Figure 3:

Mass balance for porous layer in model III-A

$$\alpha_6^i \left[\alpha_4^i \frac{\partial Y_i^s}{\partial t} - \beta_4^i \langle r_i \rangle - \left(\frac{\xi}{L}\right)^2 \frac{\partial^2 Y_i^s}{\partial z^2} - \left(\frac{\xi}{2r_h}\right)^2 \frac{\partial^2 Y_i^s}{\partial x^2} \right] + 2r_h \mathbf{n}\cdot\nabla Y_i^f = 0 \quad (53)$$

where x is again the coordinate on the periphery of a square duct. In Equation (53), $\langle r_i \rangle$ denotes the reaction rate from (52), averaged in ξ, that is, the apparent reaction rate including internal diffusion effects, and $Y_i^s = Y_i^s|_{\xi=1}$ is a function only of t, z, and x. Equations (52) and (53) solved together in this fashion do not constitute a legitimate solution to the equation for three-dimensional diffusion and reaction. The purpose of this approximation is to test for the importance of diffusion axially and peripherally. The mass transient term is included, since no additional effort is required to include it.

When infinitely fast peripheral diffusion is assumed, we get

Mass balance for porous layer in models I-A and II-A

$$\alpha_6^i \left[\alpha_{4i} \frac{\partial Y_i^s}{\partial t} - \beta_4^i \langle r^i \rangle - \left(\frac{\xi}{L}\right)^2 \frac{\partial^2 Y_i^s}{\partial z^2} \right] + 2r_h(\mathbf{n}\cdot\nabla Y_i^f) = 0 \quad (54)$$

When axial diffusion and the transient term are neglected, we get

Table 4. Description of Mathematical Models

Model	Fluid model	Diffusion and conduction peripherally in substrate and porous layer
III-A	Distributed	Finite rate
II-A	Distributed	Infinite rate (no variation peripherally)
I-A	Lumped	Infinite rate

Models with the designation A have a finite rate of axial conduction and diffusion in solid. Models without the designation A have no axial conduction or diffusion in solid.

Mass balance for porous layer in models I and II

$$2r_h(\mathbf{n}\cdot\nabla Y_i^f) = \alpha_6^i\beta_4^i\langle r_i \rangle \quad (55)$$

By comparing the results from Equations (53) to (55), the importance of axial and peripheral diffusion and the mass transient term can be determined.

The results of the various models can be compared to deduce which phenomena are important for a proper mathematical model of the catalytic converter. Table 4 lists the relevant features of the models. For example, comparison of models I-A and II-A shows the effect of a lumped parameter vs. a distributed parameter model for the fluid. Models I and II can be used to see if the same comparison between lumped and distributed fluid models holds in the absence of axial conduction in the solid. Comparison of models II-A and III-A shows the effect of peripheral variations of concentration and temperature around the substrate and porous layer, for example, along x' at $y' = 2r_h$ in Figure 4. Interestingly, models I and I-A are similar to adiabatic packed-bed reactor models, which include an external resistance between the fluid and solid catalyst. Model I is like that first solved by Liu and Amundsen (1962), and model I-A is similar to that solved by Eigenberger (1972). The calculations with these models can be related to these previous studies.

Model I-A is also very similar to the monolith converter model developed by Kuo (1973), which has been used extensively by industry. In this study, constant values of the Nusselt and Sherwood numbers are assumed, while Kuo (1973) used the axially varying Nusselt and Sherwood numbers calculated from a constant wall temperature Graetz problem. This difference is minor, and the results found with model I-A apply equally to Kuo's model. Model I-A is the same as that used by Votruba et al. (1975).

The initial conditions for model III-A are

$$T^s = T_O^s(x,z); \quad Y_i^s = Y_{i,O}^s(x,z) \quad \text{at} \quad t = 0 \quad (56)$$

At the fluid-solid interface, the following conditions apply:

$$Y_i^f = Y_i^s; \quad T^f = T^s \quad (57)$$

The boundary conditions in x are

$$\frac{\partial Y_i^s}{\partial x} = \frac{\partial T^s}{\partial x} = 0 \quad \text{at} \quad x = 0, 1 \quad (58)$$

The boundary conditions in the axial direction depend on the nature of the inlet and outlet regions, which are modeled by assuming they are ideal stirred tanks. Energy and mass balances on the fluid in the inlet region yield

$$T^f = T_O^f + 4\left(\frac{r_{hs}}{L}\right)^2 \alpha_1\alpha_5 \int_o^1 \frac{\partial T^s}{\partial z}\, dx \quad (59)$$

at $z = 0$

$$Y_i^f = Y_{i,o}^f + 4\left(\frac{\xi}{L}\right)^2 \alpha_2^i \alpha_6^i \int_o^1 \frac{\partial Y_i^s}{\partial z} dx \qquad (60)$$

Heat and mass transfer coefficients are used to describe transfer between the fluid and solid at the inlet:

$$\frac{2r_{hs}}{L}\frac{\partial T^s}{\partial z} = Nu_o(T^s - T^f) \qquad (61)$$

at $z = 0$

$$\frac{2r_{hs}}{L}\frac{\partial Y_i^s}{\partial z} = Sh_o(Y_i^s - Y_i^f) \qquad (62)$$

where Sh_o and Nu_o are defined by using $2r_{hs}$ as the characteristic length. Values of 3.5 and 5.5 have been used for Sh_o and Nu_o in the calculations, and it is found that the values of these parameters make little difference. This occurs because transfer between the fluid and wall is very fast at the inlet owing to the developing temperature profile there, so that $T^s \simeq T^f$ and $Y_i^s \simeq Y_i^f$ at the inlet regardless of the values of Nu_o and Sh_o.

A similar analysis could be applied to the outlet region; however, the following condition is used:

$$\frac{\partial T^s}{\partial z} = \frac{\partial Y_i^s}{\partial z} = 0 \quad \text{at} \quad z = 1 \qquad (63)$$

The above boundary and initial conditions can be simplified for the other models. For example, the conditions on models II-A and I-A follow by assuming that T^s and Y_i^s are constant in x. Models without axial conduction use the initial conditions

$$T^f = T_o^f; \quad Y_i^f = Y_{i,o}^f \quad \text{at} \quad z = 0 \qquad (64)$$

instead of Equations (59) to (62). Models I and I-A do not use Equation (57).

SOLUTION OF MATHEMATICAL MODEL

The solution method is based on the well-known fact that the solution of a heat transfer Graetz problem with arbitrary specified wall temperature can be expressed in terms of the solution (and various integrals) of the Graetz problem with constant wall temperature down the duct. In the monolith problem, the wall temperature down the duct is unknown, but the fluid temperature can still be written in terms of the unknown wall temperature distribution. Consequently, the temperature and concentration in the fluid can be solved directly, and only the solid equations are left to be satisfied.

To illustrate the ideas, consider a circular duct Graetz problem, Equations (1) and (2), but with the wall condition

$$T(1, z) = T_w(z) \qquad (65)$$

Sellars et al. (1956) have derived an analytical solution for this problem. Their solution can be rearranged to

$$T(x, z) = T_o - \sum_{n=1}^{\infty} \lambda_n C_n R_n(x) \int_o^z e^{\lambda_n(z-\tau)}[T_w(\tau) - T_o]d\tau \qquad (66)$$

The solution of the orthogonal collocation approximation to Equations (1), (2), and (65) is

$$T(x_i, z) = T_o + \sum_{j=1}^{N}\sum_{n=1}^{N} u_{in}u_{nj}^{-1}(1 - x_j^2)B_{j,N+1} \int_o^z e^{\lambda_n(z-\tau)}[T_w(\tau) - T_o]d\tau \qquad (67)$$

Equation (67) is a radially discrete approximation to the first N terms of the analytical solution, Equation (66). The orthogonal collocation method could be made radially continuous if desired and would then give an approximation to the Green's function for the problem. In Equation (67), the λ_n are the eigenvalues of the matrix $(1 - x_i^2)^{-1}B_{ij}$, and the u_{in} are the associated eigenvectors. The mixing cup temperature and wall heat flux are given by

$$T^M = T_o + \sum_{k=1}^{N} S_k \int_o^z e^{\lambda_k(z-\tau)}[T_w(\tau) - T_o]d\tau \qquad (68)$$

$$\left.\frac{\partial T}{\partial x}\right|_{x=1} = \frac{1}{4}\frac{dT^M}{dz} = \frac{1}{4}\sum_{k=1}^{N} S_k\left(T_w(z) - T_o + \lambda_k \int_o^z e^{\lambda_k(z-\tau)}[T_w(\tau) - T_o]d\tau\right) \qquad (69)$$

where

$$S_k = 4\sum_{i=1}^{N}\sum_{j=1}^{N} W_i(1 - x_i^2)u_{ik}u_{kj}^{-1}(1 - x_j^2)B_{j,N+1} \qquad (70)$$

In this fashion we have completely expressed the approximate solution $T_i = T(x_i, z)$ [and hence $T(x, z)$] in terms of the wall temperature $T_w(x)$.

For more complicated geometries, the details become more complex, but the ideas are similar and are applied here to the rectangular geometry. Only the temperature equations are given in detail. The mass balances follow by analogy. Orthogonal collocation applied to Equations (33) and (36) yields

$$8\left(\frac{r_h}{a}\right)^2\left[\sum_{k=1}^{N} B_{ik}^x G_{kj} + \left(\frac{1}{b}\right)^2 \sum_{l=1}^{M} B_{jl}^y G_{il}\right] = -1 \qquad (71)$$

$$\frac{G_{ij}}{\langle G\rangle}\frac{dT_{ij}}{dz} = 8\left(\frac{r_h}{a}\right)^2\left[\sum_{k=1}^{N+1} B_{ik}^x T_{kj} + \left(\frac{1}{b}\right)^2 \sum_{l=1}^{M+1} B_{il}^y T_{il}\right] \qquad (72)$$

Here the boundary and initial conditions are taken as

$$T(x, y, 0) = T_o, \quad T(x, 1, z) = h(x, z), \quad T(1, y, z) = g(y, z) \qquad (73)$$

leading to collocation approximations:

$$T_{ij}(0) = T_o, \quad T_{i,M+1} = h(x_i, z), \quad T_{N+1,j} = g(y_j, x) \qquad (74)$$

In these formulas, $T_{ij}(z) = T(x_i, y_j, z)$. The fluxes on the walls are

$$\text{on } y = 1: \quad 2r_h\mathbf{n}\cdot\nabla T\Big|_{x_i, y_{M+1}} = \frac{1}{b}\left(\frac{2r_h}{a}\right)\sum_{j=1}^{M+1} A^y{}_{M+1,j}T_{ij} \qquad (75)$$

$$\text{on } x + 1: \quad 2r_h\mathbf{n}\cdot\nabla T\Big|_{x_{N+1}, y_j} = \frac{2r_h}{a}\sum_{i=1}^{N+1} A^x{}_{N+1,i}T_{ij} \qquad (76)$$

The above Equations (71) and (72) involve an unknown matrix T_{ij}. The collocation points are renumbered

by a single index so that these equations can be written as

$$\sum_{j=1}^{N_1} F_{ij}{}^s G_j = -1 \tag{77}$$

$$\frac{G_i}{\langle G\rangle}\frac{dT_i}{dz} = \sum_{j=1}^{N_1} F_{ij}{}^s T_j + \sum_{j=1}^{N_2} F_{ij}{}^c f_j \tag{78}$$

In these equations, $\{f_j\}$ are the values of $h(x_i, z)$ and $g(y_j, z)$ numbered in sequence around the periphery; hence, $N_2 = N + M$. $N_1 = N \times M$ is the total number of interior collocation points. For all models except model III-A, $f_j = f_i$ for all i and j, since the conditions are the same at all points on the periphery in the other models. For the simpler models, Equation (78) can be simplified to the same form but with $N_2 = 1$.

Equation (78) is identical in form to the equations for the circular duct, Equation (12), with wall condition (65). Other geometries also yield equations of the same form as Equation (78).

The solution is

$$T_i = T_O + \sum_{k=1}^{N_1}\sum_{j=1}^{N_1}\sum_{l=1}^{N_2} u_{ik}u_{kj}{}^{-1}\frac{\langle G\rangle}{G_j}F_{jl}{}^c\int_o^z e^{\lambda_k(z-\tau)}[f_l(\tau) - T_o]d\tau \tag{79}$$

where λ_k are the eigenvalues, and the U_{ik} are the associated eigenvectors of $F_{ij}{}^s\ \langle G\rangle/G_i$. The mixing cup temperature is given by

$$T^M = T_O + \sum_{k=1}^{N_1}\sum_{l=1}^{N_2}\hat{S}_{kl}\int_o^z e^{\lambda_k(z-\tau)}[f_l(\tau) - T_O]d\tau \tag{80}$$

where

$$\hat{S}_{kl} = \sum_{i=1}^{N_1}\sum_{j=1}^{N_1} W_i{}^s u_{ik}u_{kj}{}^{-1}\frac{G_i}{G_j}F_{jl}{}^c \tag{81}$$

The flux on the boundary is obtained from Equations (75) and (76), which are rearranged from a form with T_{ij} to one with T_j:

$$2r_h\mathbf{n}\cdot\nabla T\Big|_j = \sum_{i=1}^{N_1} H_{ji}{}^S T_i + \sum_{i=1}^{N_2} H_{ji}{}^C f_i, \quad j = 1, \ldots, N_2 \tag{82}$$

The use of Equation (79) permits this to be written as

$$2r_h\mathbf{n}\cdot\nabla T|_j = \sum_{i=1}^{N_2} H_{ji}{}^C(f_i - T_O) + \sum_{k=1}^{N_1}\sum_{l=1}^{N_2} R_{jk}{}^F R_{kl}{}^S\int_o^z e^{\lambda_k(z-\tau)}[f_l(\tau) - T_o]d\tau \tag{83}$$

where

$$R_{jk}{}^F = \sum_{i=1}^{N_1} H_{ij}{}^S u_{ik}, \quad R_{kl}{}^S = \sum_{j=1}^{N_1} u_{kj}{}^{-1}\frac{\langle G\rangle}{G_j}F_{jl}{}^C \tag{84}$$

The appropriate quantities λ, u, $\hat{S}$, H, F, G are calculated for the Graetz problem in order to use them in the equations for the monolith.

The fluid balance for the monolith, Equation (44), differs from Equation (36) only by the factor α_1. The mixing cup temperature from Equation (44) is then derived by modifying Equation (80):

$$T^M(z) = T_O{}^f + \sum_{k=1}^{N_1}\sum_{l=1}^{N_2}\hat{S}_{kl}\int_o^z e^{\alpha_1\lambda_k(z-\tau)}[T_l{}^s(\tau) - T_o]\alpha_1 d\tau \tag{85}$$

The normal flux is likewise

$$2r_h\mathbf{n}\cdot\nabla T|_{j,z} = \sum_{i=1}^{N_2} H_{ji}{}^c(T_i{}^s - T_O{}^f) + \sum_{k=1}^{N_1}\sum_{l=1}^{N_2} R_{jk}{}^F R_{kl}{}^A\int_o^z e^{\alpha_1\lambda_k(z-\tau)}[T_l{}^s(\tau) - T_o{}^f]\alpha_1 d\tau \tag{86}$$

We note that in order to apply this method we must assume that α_1 (and $\alpha_2{}^i$) are constant in z.

The problem is discretized in the axial direction by approximating $T_l{}^s(z)$ by using Lagrange interpolation over subregions or elements of equal length. Expansion of the Lagrange interpolating polynomial gives the standard collocation interpolation formula (Finlayson, 1972, p. 101). In the m^{th} element with coordinate $\xi = 0 \to 1$, we get

$$T_l{}^s|_\xi{}^m = \sum_{i=1}^{N_4} T^s|_{il}{}^m \sum_{j=1}^{N_4} Q_{ji}{}^{-1}\xi^{j-i} \tag{87}$$

where $T^s|_{il}{}^m = T_l{}^s|_{\xi i}{}^m$ and the points ξ_i are conveniently taken as Gaussian quadrature base points.

Equations (85) and (86) can be used after a method of calculating the integrals is devised.

For each eigenvalues λ_k, we calculate a quadrature weight

$$W_{kji} = \sum_{l=1}^{N_4} Q_{li}{}^{-1}\left(\frac{\alpha_1}{N_5}\right)\int_o^{\xi_j} e^{\alpha_1\lambda_k(\xi_j-\tau)/N_5}\tau^{l-1}d\tau \tag{88}$$

In these formulas, the axial direction has been divided into N_5 elements, each having N_4 collocation points. Equation (86) can then be written as

$$2r_h\mathbf{n}\cdot\nabla T|_{r,n}{}^m = \sum_{i=1}^{N_2} H_{ni}{}^C(T^s|_{ri}{}^m - T_O{}^f) + \sum_{k=1}^{N_1}\sum_{l=1}^{N_2} R_{nk}{}^f R_{kl}{}^s\int_o^{(m-1)/N_5} e^{\alpha_1\lambda_k\left(\frac{m-1}{N_5}-\tau\right)}[T_l{}^s(\tau) - T_O{}^f]\cdot\alpha_1 d\tau + \sum_{i=1}^{N_4}\sum_{j=1}^{N_2}\sum_{k=1}^{N_1} R_{nk}{}^F R_{kj}{}^S W_{kri}T^s|_{ij}{}^m \tag{89}$$

where

$$T^s|_{rn}{}^m = T\left(x_n, y_n, \frac{m-1}{N_5} + \xi_r\right) \tag{90}$$

is the wall temperature, at the r^{th} axial collocation point in the m^{th} axial element, and at the n^{th} peripheral position. These equations are rewritten as

$$2r_h\mathbf{n}\cdot\nabla T|_{rn}{}^m = \sum_{i=1}^{N_4}\sum_{j=1}^{N_2} F_{rnij}T^s|_{ij}{}^m + G_{rn}{}^m \tag{91}$$

The matrix F does not vary from element to element. Equation (91) completes the specification of the normal flux at any axial collocation point r in element m and any peripheral position (n) in terms of the wall temperature at the axial collocation points r in element m and the set of peripheral position $(j = 1, \ldots, N_2)$. When heat conduction peripherally is very fast (all models except III-A), $N_2 = 1$.

By means of Equations (85) and (86) or (91), the fluid equation for models II, II-A, III-A are essentially solved. Equation (91) is substituted into Equation (49) for model III-A. The peripheral Laplacian is approximated by orthogonal collocation, while the axial Laplacian term uses orthogonal collocation on finite elements as well as the continuity conditions between elements (Carey and Finlayson, 1975):

$$\left.\frac{\partial^2 T^s}{\partial z^2}\right|_{rn}^{m} = \frac{1}{(\Delta z)^2}\sum_{j=1}^{N_4} B_{nj}{}^z T^s \Big|_{rj}^{m}$$

$$\left.\frac{\partial^2 T^s}{\partial x^2}\right|_{rn}^{m} = \sum_{j=1}^{N_2} B_{rj}{}^x T^s \Big|_{jn}^{m} \qquad (92)$$

The result is a set of ordinary differential equations for T^s at the axial and peripheral collocation points. This set of equations is solved for a transient solution by using a backward Euler method, with a Picard, or successive substitution method of iteration applied sequentially on each element. Iteration parameters are included, and guidelines for the crucial choice of these iteration parameters is given elsewhere (Young, 1974). Stability of the iteration process is enhanced by large iteration parameters, but computation times are then longer. If only a steady state result is desired, the coefficient of the time derivatives is set to zero, for example, $\alpha_3 = 0$. This corresponds to taking a time step Δt of infinity. The iteration to steady state solutions did not converge for all cases, so the transient case was calculated to steady state. The calculations proceeded element by element. The solution at all collocation points in the first element was found by successive iterations, and then each successive element down the duct was solved in turn. If there is no axial conduction in the wall, such a sweep down the duct completes the steady state solution or one-time step in the transient solution. If axial conduction is present, then what happens at the outlet influences what happens at the inlet, so that several more sweeps must be made down the duct before convergence is obtained for a single time step or steady state. Since the full set of equations represents about 1 000 coupled nonlinear equations, the difficulties in the iteration method are not surprising.

Model II calculations could be done for a circular cross section with three radial collocation points (N_1), and for severe cases 1 001 points were used axially ($N_4 = 3$, $N_5 = 500$). When model II-A was used, the number of collocation points per element was from 5 to 7 (N_4), and from 20 to 80 elements (N_5) were used. The number of collocation points interior to the fluid, hence the number of eigenvalues λ_k calculated, ranged from $N_1 = 4$, 6, 15, and 15 for the cross sections having the shape of a circle, square, rectangle, or trapezoids. Computation times ranged from 10 to 40 s for steady state solutions on a CDC 6400 computer, depending on the complexity of the geometry and the difficulty of the particular steady state problem being calculated. For model III-A, with peripheral variations of temperature and concentration and a square cross section, typical values used were $N_1 = 6$ for the number of interior collocation points and $N_2 = 3$ for the number of boundary points. Owing to the symmetry apparent in Figure 4, only a few collocation points were needed to obtain accurate solutions. Computation times for model III-A for the square ranged from 32 to 250 s on the same machine.

In the transient calculations, the step size ranged from 0.125 to 1 s during the transient. The computation time depended drastically on the severity of the solution being calculated. With model II, one solution took 50 s of computation to calculate 38 s of the model solution, whereas a more severe case took 900 s of computation for 14 s of real time. Model II-A calculations were from four to six times less than model II calculations and typically required from ten to fifteen times real time, but a complete transient in real time can take place in as little as 25 s. Model III-A typically required four times the computation time of model II-A, or fifty times real time.

That solutions could be obtained at all is due largely to the use of the eigenvalue technique. A typical steady state solution to models II-A or III-A with $N_4 = 7$ and $N_5 = 25$ requires the solution of 302 and 906 simultaneous algebraic equations, respectively. Had the eigenvalue technique not been used, then for square geometry and $N_1 = 6$, the two models would have required the solution of 2 114 and 2 718 simultaneous algebraic equations.

NOTATION

a = duct dimension m, constant in Equation (43)
A_c = total converter frontal area, m^2
A_{ij} = orthogonal collocation matrix for approximating a first derivative
b = rectangle or trapezoid aspect ratio
B_{ij} = orthogonal collocation matrix for approximating a single dimension Laplacian operator
c = trapezoid aspect ratio
C = total molar concentration ρ/M_w, 0.0151 kg mole/m^3
$C_p{}^f$ = molar heat capacity of fluid, 3.140×10^4 J/kg mole °K
$C_p{}^s$ = mass heat capacity of solid, J/kg K, $\rho^s C_p{}^s = 4.14 \times 10^5$ J/m^3 °K
d = converter wall thickness, m
$D_i{}^f$ = effective molecular fluid diffusivity for component i, m^2/s
$D_i{}^s$ = effective porous solid diffusivity for component i, m^2/s, $D_i{}^s = 0.05\ D_i{}^f$
$\mathbf{e}_x$ = unit vector in x direction
$\mathbf{e}_y$ = unit vector in y direction
f = general function
fRe = friction factor Reynolds number product $(8r_h{}^2 C\ dP/dz')/\langle G' \rangle \mu$
$F_{ij}{}^S$ = orthogonal collocation matrix for the approximation of a two-dimensional Laplacian operator and operating on the interior point values
$F_{ij}{}^C$ = orthogonal collocation matrix for the approximation of a two-dimensional Laplacian operator and operating on the boundary point values
g = general function or a function describing a two-dimensional region
$\hat{g}$ = function defined in Equation (28)
G' = molar flux, kg mole/sm^2
G = dimensionless molar velocity, $G'\mu/(8r_h{}^2 C dp/dz')$
h^* = heat transfer coefficient, J/sm^2 °K
h = general function or a function describing a two-dimensional region
$\hat{h}$ = function defined in Equation (28)
H_i = enthalpy change associated with the generation of mole of component i, 3.37×10^8 J/(kg mole CO + 1/3 kg mole H_2)
$H_{ij}{}^S$ = orthogonal collocation matrix for the approximation of a normal gradient at a boundary and operating on the interior point values
$H_{ij}{}^C$ = orthogonal collocation matrix for the approximation of a normal gradient at a boundary and operating on the boundary point values
k^* = mass transfer coefficient, m/s
k = thermal conductivity, J/smk
k^s/k^f = ratio of solid to fluid thermal conductivity, 25
l = line coordinate on the periphery of a two-dimensional region
L = converter length, m

$L_i(x)$ = Lagrange interpolating polynomial
M = order of approximation
M_w = average molecular weight of the fluid, 28.8 kg/kg mole
$\mathbf{n}$ = unit normal vetor point outward from a two-dimensional region
N = order of approximation
N_1 = number of collocation points or eigenvalues for the fluid
N_2 = number of boundary (peripheral) collocation points
N_4 = number of axial collocation points in an element (including boundary points)
N_5 = number of axial elements
Nu = Nusselt number, $4r_h h^*/k^f$
$<Nu>$ = Nusselt number averaged around the periphery
Nu_∞ = asymptotic Nusselt number
Nu_o = Nusselt number for heat exchange between the incoming fluid and the front face of the converter solid, $2r_{hs}h^*{}_o/k^s$
P = total pressure, N/m^2
Pr = Prandtl number of fluid, $\mu C_p{}^f/k^f M_w$, 0.7.
Pe_h = Peclet number for heat, $PrRe$
$Pe_m{}^i$ = Peclet number for component i, Sc_iRe
$P_N(x)$ = orthogonal polynomial of N^{th} degree in x
r_i = rate of generation of component i, kg mole/sm^3
r_h = hydraulic radius of a duct, the duct open area divided by the duct perimeter, m
r_{hs} = hydraulic radius of the solid in the converter, the solid area divided by the fluid-solid interfacial length, or the solid volume divided by the superficial surface area, or $r_{hs} = (1-\epsilon)r_h/\epsilon$, m
$R_{jk}{}^F$ = matrix for the flux around the periphery of a duct, defined by Equation (84).
$R_{kl}{}^S$ = matrix for the flux around the periphery of a duct, defined by Equation (84).
Re = Reynolds number, $4r_hG'M_w/\mu$, 1900G std. (m^3/s)
Q_{ij} = interpolation matrix in collocation method
S = surface area in two dimensional quadrature formula
Sc_i = Schmidt number, $\mu/(\rho D_i{}^f)$, 0.7
$S_k, \hat{S}_{kj}$ = coefficients for the mixing cup temperature in a wall temperature specified Graetz problem, defined by Equations (70) and (81).
S_c = converter superficial surface area, $\epsilon A_c L/r_h$, m^2
Sh = Sherwood number, $4r_hk^*/D^f$
Sh_o = Sherwood number for mass interchange between the incoming fluid and the front face of the converter solid, $2r_{hs}k_o{}^*/D^s$
t = time, s
T = temperature, °K
u_{ik} = the eigenvector associated with the k^{th} eigenvalue of the wall temperature specified Graetz problem
W_i = quadrature weight for the i^{th} base point
x = dimensionless x' coordinate
y = dimensionless y' coordinate
Y_i = mole fraction of component i
z = dimensionless axial coordinate, $z'/(2r_hPe)$ or z'/L

Greek Letters

α_1 = dimensionless thermal converter length, $L/2r_hPe_h = 0.02/\hat{G}$ (std. m^3/s)
$\alpha_2{}^i$ = dimensionless mass converter length for component i, $L/2r_hPe_m{}^i = 0.02/\hat{G}$ (std. m^3/s)
α_3 = time constant, $\rho^sC_p{}^sr_{hs}{}^2/k^s = 0.0224$ s
$\alpha_4{}^i$ = time constant for component i, $\epsilon_s\zeta^2/D_1{}^s$, $\alpha_4{}^{CO} = 1.59 \times 10^{-5}$ s
α_5 = ratio of fluid to solid resistance to heat transfer $(k^s/k^f)(2r_h/r_{hs})$, 100
$\alpha_6{}^i$ = ratio of fluid to solid resistance to mass transfer, $(D_i{}^s/D_i{}^f)(2r_h/\zeta)$, 2
$\beta_4{}^i$ = mass reaction coefficient, $\zeta^2/CD_i{}^s$, 2.02×10^{-10} m^3 s/kg mole for CO
$\beta_5{}^i$ = thermal reaction coefficient, $H_i2r_h\zeta/k^f$, 4.35×10^{-6} m^3
ϵ = void fraction of converter, or fractional open area, $r_h/(r_h + r_{hs})$
ϵ_s = void fraction of the catalytic layer
ζ = thickness of the catalytic layer, m
η = dimensionless transformed coordinates
λ_k = k^{th} eigenvalue for the wall temperature specified Graetz problem
μ = viscosity of gas, 3.57×10^{-5} kg/ms
ξ = dimensionless tranformed coordinate
ρ = density, kg/m^3
τ = dummy variable of integration

Subscripts and Superscripts

S = value for the interior of the region
C = value for the boundary of the region
f = fluid value
M = mixing cup average value
O = initial or inlet value
s = solid value
w = wall value
$l, g, h, \xi, \eta, x, y, z$ = superscripts on quadrature formula or collocation matrices associated with line integral, functions, or dimensions
$'$ = dimensional quantity
m = element number
$\hat{m}$ = number of independent chemical species
i, j, k, l, r = collocation point
$\{f\}$ = average of f on boundary of two-dimensional duct
$<f>$ = average of f in cross section of two-dimensional duct

LITERATURE CITED

Bird, R. B., W. E. Stewart, and E. N. Lightfoot, *Transport Phenomena*, Wiley, New York (1960).

Carey, G. F., and B. A. Finlayson, "Orthogonal Collocation on Finite Elements," *Chem. Eng. Sci.*, **30**, 587-596 (1975).

Eigenberger, G., "On the Dynamic Behavior of the Catalytic Fixed-Bed Reactor in the Region of Multiple Steady States. I. The Influence of Heat Conduction in Two Phase Models," *Chem. Eng. Sci.*, **27**, 1909-1915 (1972).

Elnashaie, S. S. E., and D. L. Cresswell, "Dynamic Behavior and Stability of Non-Porous Catalyst Particles," *Chem. Eng. Sci.*, **28**, 1387-99 (1973).

Ferguson, N. B., "Orthogonal Collocation as a Method of Analysis in Chemical Reaction Engineering," Ph.D. thesis, Univ. Wash., Seattle (1971).

———, and B. A. Finlayson, "Transient Modeling of a Catalytic Converter to Reduce Nitric Oxide in Automobile Exhaust," *AIChE J.*, **20**, 539-550 (1974).

Finlayson, B. A., *The Method of Weighted Residuals and Variational Principles*, Academic Press, New York (1972).

Hegedus, L. L., "Temperature Excursions in Catalytic Monoliths," *General Motors Report GMR-1712, PCP-30* (1974).

Hennecke, D. K., "Heat Transfer by Hagen-Poiseuille Flow in the Thermal Development Region with Axial Conduction," *Wärme—und Staffübertragung*, **1**, 177-84 (1968).

Howitt, J. S., and T. C. Sekella, "Flow Effects in Monolithic Honeycomb Automotive Catalytic Converters," *Soc. Auto. Eng. Trans.*, 740244 (1974).

Krylov, V. I., *Approximate Calculation of Integrals*, Macmillan, New York (1962).

Knudsen, J. G., and D. L. Katz, *Fluid Dynamics and Heat Transfer*, McGraw-Hill, New York (1958), p. 105.
Kuo, J. C. W., Private communication (1973).
Lemme, C. D., and W. R. Given, "Flow Through Catalytic Converters—An Analytical and Experimental Treatment," *Soc. Auto. Eng. Trans.*, 740243 (1974).
Liu, S. L., and N. R. Amundson, "Stability of Adiabatic Packed Bed Reactors. An Elementary Treatment," *Ind. Eng. Chem. Fundamentals*, **1**, 200-8 (1962).
Michelsen, M. L., and J. Villadsen, "The Graetz Problem with Axial Heat Conduction," *Intern. J. Heat Mass Transfer*, **17**, 1391-1402 (1974).
Morgan, C. R., D. W. Carlson, and S. E. Voltz, "Thermal Response and Emission Breakthrough of Platinum Monolithic Catlytic Converters," Soc. Auto. Eng., paper 730569 (1973).
Sellars, J. R., M. Tribus, and J. S. Klein, "Heat Transfer to Laminar Flow in a Round Tube or Flat Conduit—the Graetz Problem Extended," *Trans. ASME*, **78**, 441-8 (1956).
Shah, R. K., and A. L. London, "Laminar Flow Forced Convection Heat Transfer and Flow Friction in Straight and Curved Ducts—A Summary of Analytical Solutions," *Tech. Rep. No. 75*, Dept. Mech. Eng., Stanford Univ., Calif. (1971).
Smith, J. M., *Chemical Engineering Kinetics*, 2 ed., McGraw-Hill, New York (1970).
Sørensen, J. P., and W. E. Stewart, "Computation of Forced Convection in Slow Flow Through Ducts and Packed Beds—I. Extensions of the Graetz Problem," *Chem. Eng. Sci.*, **29**, 811-817 (1974).
———, "Computation of Forced Convection in Slow Flow Through Ducts and Packed Beds—III. Heat and Mass Transfer in a Simple Cubic Array of Spheres," *ibid.*, 827-832 (1974).
Sørensen, J. P., E. W. Guertin, and W. E. Stewart, "Computational Models for Cylindrical Catalyst Particles," *AIChE J.*, **19**, 969-75 (1973).
Stroud, A. H., *Approximate Calculation of Multiple Integrals*, Prentice-Hall, Englewood Cliffs, N. J. (1971).
Stroud, A. H., and D. Secrest, "Gaussian Quadrature Formulas," Prentice-Hall, Englewood Cliffs, N. J. (1966).
Villadsen, J. V., and W. E. Stewart, "Solution of Boundary-Value Problems by Orthogonal Collocation," *Chem. Eng. Sci.*, **22**, 1483-1501 (1967).
Votruba, J., J. Sinkule, V. Hlaváček, and J. Skřivánek, "Heat and Mass Transfer in Monolithic Honeycomb Catalysts—I," *ibid.*, **30**, 117-123 (1975).
Young, L. C., "The Application of Orthogonal Collocation to Laminar Flow Heat and Mass Transfer in Monolith Converters," Ph.D. thesis, Univ. Wash., Seattle (1974).
———, and B. A. Finlayson, "Axial Dispersion in Nonisothermal Packed Bed Chemical Reactors," *Ind. Eng. Chem. Fundamentals*, **12**, 412-422 (1973).
———, "Mathematical Modeling of the Monolith Converter," Third International Symposium on Chemical Reaction Engineering—II, *Adv. Chem. Soc.*, **133**, 629 (1974).

Manuscript received August 26, 1975; revision received December 1, and accepted December 4, 1975.

Mathematical Models of the Monolith Catalytic Converter:

Part II. Application to Automobile Exhaust

Calculations are done for a series of mathematical models for a monolith catalytic converter to oxidize carbon monoxide in automobile exhaust. Phenomena studied include axial conduction in the wall, diffusion and conduction in the gas in a transverse direction perpendicular to the flow direction, multiple steady states, and transients giving wall temperatures exceeding the adiabatic temperature.

LARRY C. YOUNG

and

BRUCE A. FINLAYSON

Department of Chemical Engineering
University of Washington
Seattle, Washington 98195

SCOPE

For better or for worse, the use of catalytic converters to reduce automobile emissions of carbon monoxide and hydrocarbons has become a reality. Two types of catalytic converters are used for this application: packed beds and monoliths. The present study is concerned with mathematical models for the monolith converter. The simplest model which will give realistic predictions is determined, and the model calculations illustrate the important phenomena occurring in the device.

Although considerable attention has been devoted to modeling packed-bed converters (Wei, 1975), little published information is available on modeling monolith converters. Kuo (1973) developed a lumped parameter model for the monolith converter, which has been used by eight automobile and oil companies. Votruba et al. (1975) have also presented a similar model. Both these models include axial conduction in the wall. Hegedus (1974) neglects axial conduction. In a preliminary study, Young and Finlayson (1974) proposed and solved two models for the monolith, which cast some doubt on the validity of the simpler models. The essential question is whether or not to include diffusion and conduction in the fluid in a transverse direction perpendicular to the flow (and duct) axis, as did Young and Finlayson, or whether a simple lumped parameter model of this phenomenon, with specified Nusselt and Sherwood numbers,

Larry C. Young is with Amoco Production Company, Tulsa, Oklahoma.

is sufficient, as was done by Kuo, by Hegedus, and by Votruba et al.

In the present study, calculations are done for a series of mathematical models. Comparison of the results enables the choice of the simplest model which can be used for realistic predictions. The question of diffusion and conduction perpendicular to the flow axis is considered, as well as the importance of axial conduction in the wall and peripheral diffusion and conduction in the wall around the duct. The effect on the reaction rate of diffusion limitations in the porous substrate is also included. The results provide a complete study of the types of phenomena occurring in monolith devices.

One of the important limitations to the use of monolith reactors in automobiles is peak overtemperatures which cause the solid walls to melt or deform, which eventually leads to the destruction of the device (Morgan, et al., 1973). Calculations are done to investigate this phenomenon and its dependence on transverse diffusion and conduction in the fluid, axial conduction, and the presence of significant amounts of hydrogen. Model calculations also illustrate the effect of different duct shapes on the performance of the converter. Steady state and transient simulations are included, with transient models being especially important for application to automobile exhaust.

CONCLUSIONS AND SIGNIFICANCE

The most important transport phenomenon which must be included in a model of the monolith reactor is the diffusion and conduction of species and energy in the fluid in a transverse direction perpendicular to the duct axis. Lumped parameter models with Nusselt and Sherwood numbers assigned a priori do not suffice unless multiple steady states are not predicted. Unfortunately, for realistic conditions for treatment of automobile exhaust, multiple steady states are predicted to occur, and lumped parameter models are unsuitable.

Axial conduction in the solid is sometimes important, and its inclusion in the model tends to reduce the temperature gradient at the point where the reaction lights off and to reduce the peak overtemperature during transient and steady state simulations. Both effects tend to shorten the computation time for transient simulations when axial conduction is included rather than excluded. Peripheral variations of temperature and concentration around the duct at a given axial location are predicted to occur, but the effect on the overall performance of the converter is negligible. If hydrogen is modeled as a separate species, rather than relating it strictly to the carbon monoxide concentration, the peak overtemperatures are larger, but still not sufficient to cause melting of the converter during normal operation of the automobile.

MODEL DEVELOPMENT

The monolith converter consists of a number of cells or ducts through which the exhaust gas flows. A diagram of a single square cell is shown in Figure 1. Other cell shapes are possible, and those considered in this study are shown in Figure 2.

The monolith converter consists of the three regions shown in Figure 1: a laminar flow region, a porous catalytic layer, and a relatively nonporous substrate. A cell is typically 1.3 mm wide, the catalytic layer is approximately 0.025 mm thick, and the substrate is typically 0.25 mm thick. A typical converter will contain thousands of these cells. After an initial length in which the velocity profile develops, the fluid flows in laminar flow through each cell. The reactants in the fluid diffuse to the wall and into the catalytic layer, where the reaction occurs; the heat generated and the reaction products diffuse back to the fluid and are carried downstream. All of the models studied here embody the assumption that the velocity profile of the fluid is fully developed

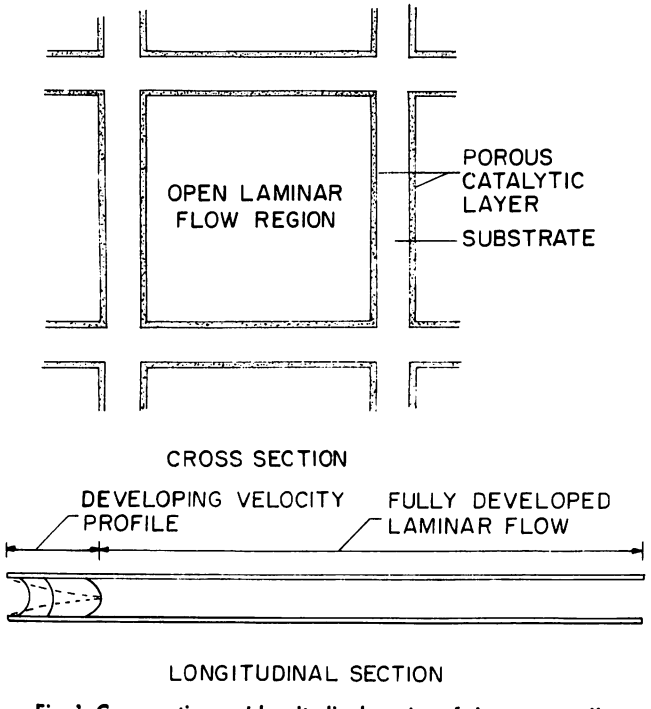

Fig. 1. Cross section and longitudinal section of the square cell.

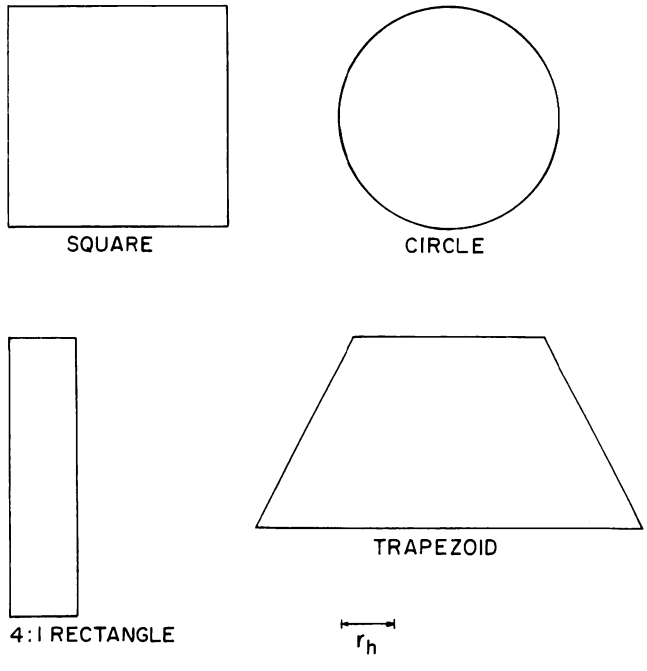

Fig. 2. Cross sections used in this study. Compared at constant r_h.